



---

**Research article**

## **Platoon-based collision-free control for connected and automated vehicles at non-signalized intersections**

**Jian Gong<sup>1</sup>, Yuan Zhao<sup>2</sup>, Jinde Cao<sup>3,\*</sup> and Wei Huang<sup>1</sup>**

<sup>1</sup> Intelligent Transportation System Research Center, Southeast University, Nanjing 210096, China

<sup>2</sup> College of Information Engineering, Dalian University, Dalian 116622, China

<sup>3</sup> School of Mathematics, Southeast University, Nanjing 210096, China

**\* Correspondence:** Email: jdcao@seu.edu.cn.

**Abstract:** This paper proposes a distributed collision-free control scheme for connected and automated vehicles (CAVs) at a non-signalized intersection. We first divide an intersection area into three sections, i.e., the free zone, the platoon zone, and the control zone. In order to enable the following vehicles to track the trajectory of their leading vehicle in the platoon zone and the control zone, as well as to guarantee the desired distance between any two adjacent vehicles, the distributed platoon controllers are designed. In the control zone, each vehicular platoon is taken as a whole to be coordinated via an intersection coordination unit (ICU). To avoid collision between each pair of the conflicting platoons approaching from different directions, a platoon-based coordination strategy is designed by scheduling the arrival time of each leading vehicle of different platoons. Specially, considering traffic efficiency and fuel economy, the optimal control problem of the leading vehicle is formulated subject to the constraint of allowable minimum arrival time, which is derived from coordination with other approaching platoons. The Pontryagin Minimum Principle (PMP) and phase-plane method are applied to find the optimal control sequences. Numerical simulations show the effectiveness of this scheme.

**Keywords:** connected automated vehicles; intersection control; platoon control; collision avoidance; trajectory optimization

---

### **1. Introduction**

Increasing urban traffic congestion seriously affects the social progress and the quality of people's daily lives, since it causes adverse economic impact, waste of fuel and death of civilians. As the bottlenecks of traffic flow, intersections witness the occurrence of traffic congestion and a large number of traffic accidents every day. According to [1], more than 20% of fatal traffic accidents occurred at intersections during 2001–2010 in the European Union. A similar ratio was found in the United

---

States [2]; about 40% of the crashes and 21.5% of the traffic fatalities happened at intersections during the comparable period. Hence, effective management and control of intersections play a crucial role in alleviating the traffic pressure and the frequency of traffic accidents.

In the past few decades, researchers have made great efforts to improve the traffic efficiency at signalized intersections, such as SCOOT [3], SCAT [4] and TRANSYT [5]. These systems improve traffic throughput at intersections to some extent through rough traffic estimation. With the prevalence of intelligent transportation systems (ITS), accurate traffic queue estimation using vehicular communication achieves more efficient real-time signal control [6]. There exist numerous results on adaptive traffic signal control, e.g., [7, 8], which focus on optimizing the phase and timing of signal light to improve traffic efficiency. However, inconveniences of frequent stops and idling are still inevitable in the traditional traffic signal paradigm. Non-signalized intersections have no signal light or any other operating device to regulate traffic flow. Traditionally, drivers need to observe and estimate the acceptable vehicle clearance through visual judgment for safe crossing. Nowadays, by using Vehicle-to-Vehicle (V2V) and Vehicle-to-Infrastructure (V2I) communication technologies to construct a reliable and real-time connected vehicle (CV) environment, it is possible for vehicles to cross intersections cooperatively, safely and efficiently. On this basis, connected automated vehicles (CAVs) can provide shorter vehicular gaps and faster responses, resulting in tremendous potential to improve the capacity, mobility and traffic safety at non-signalized intersections.

Recently, some results on cooperative intersection management under CV environment have been given in the literature. Two main methods are applied to the management of automated intersections, cooperative resource reservation and trajectory planning, as categorized in [6]. In the framework of the reservation-based approach, vehicles need to reserve the tiles on their planned route for non-conflicting time and space slots. If the slots are available, the host vehicle can cross the intersection safely. Otherwise, the vehicle continues sending requests to the intersection controller until it is authorized to pass. For instance, a reservation-based intersection control mechanism was proposed to alleviate traffic congestion at an isolated intersection [9]. The results showed it outperforming the method using traffic light in the simulation. The extended work was developed in [10], where a reservation-based multi-agent system was built by treating vehicles and intersections as autonomous agents. The intersection manager granted or rejected the request of the vehicle agent depending on whether it conflicted with the previous reservations. In [11], a timed net-based control policy was proposed to deal with resource reservation, where the passing sequences were generated by minimizing the instant queue length. The trajectory planning approaches mainly focus on predicting the trajectory of potential conflict vehicles from different directions, and then scheduling the time-based velocity or acceleration profiles of the host vehicle. In [12], a cooperation driving pattern of blind crossing was studied by using a spanning tree to represent the scheduling of collision-free movements of vehicles. In [13], a cooperative intersection control algorithm was proposed to eliminate potential overlaps of vehicles' trajectories. In [14], a global coordination scheme was presented by using the model predictive control method. The optimal trajectories were obtained to prevent each pair of conflicting vehicles from reaching the cross-collision point at the same time. In addition, improvement of driving experience quality was considered in [15], and a relevant autonomous intersection control mechanism was proposed with a comprehensive performance index, involving the vehicle jitter, the acceleration and the desired velocity. In the aforementioned works, the reservation-based approach only considered collision avoidance but ignored fuel efficiency. Moreover, frequent requests for each vehicle cause heavy communication

burden, especially in the high-density traffic condition. For the trajectory planning approach, most of the previous results simply concerned the scheduling of the crossing sequence, but they paid little attention to the implementation of the crossing sequence on a vehicular dynamics level. To enhance practicability of the intersection coordination system, it is necessary to consider fuel consumption, communication burden, and vehicular dynamics simultaneously.

In the past few decades, the automated vehicular platoon has attracted extensive attention due to its significant potential to improve transportation efficiency, fuel economy and road safety [16]. An automated platoon enables the vehicles in the same group to move at a consistent speed while maintaining a desired gap. Many issues of platoon control have been discussed and studied, such as vehicular dynamics modeling [17], the choice of spacing policies [18], communication topologies [19,20], network factors [21], and string stability [22]. Advanced control methods have also been applied for better performance, such as sliding-mode control [23],  $H_\infty$  control [24] and model predictive control [25]. Furthermore, facilitated by the above techniques, the concept of a virtual platoon was introduced into the cooperative intersection control [26,27], where vehicles clustering at the intersection in 2 dimensions were transformed to a virtual platoon in the virtual 1-dimension lane by the rotating projection. These results just focus on regulating the vehicular movement to cross the intersection safely. However, direct optimization of vehicle trajectory for acquiring better performance, such as fuel economy and traffic efficiency, has remained challenging.

In this paper, we propose a distributed collision-free control scheme for CAVs to pass through the non-signalized intersection without collision. In particular, we consider each vehicular platoon as a whole instead of an individual vehicle. A novel cooperative framework of CAVs is designed by integrating tracking control of the following vehicles and trajectory optimization of the leading vehicle to take full advantage of the road space. The expansion area of the intersection is divided into the free zone, the platoon zone and the control zone, where the specific vehicle movements are permitted in the respective zones. First, CAVs aim at forming automated platoons in the platoon zone and the control zone. To this end, a linearized vehicle longitudinal dynamic model is constructed by using the exact feedback linearization technique. A useful stable platoon controller design method is proposed to make all the following vehicles track the trajectory of their leading vehicle. Second, on that basis, the trajectory of the leading vehicle in each platoon is coordinated and planned via the intersection coordination unit (ICU). By scheduling the arrival time of each leading vehicle, a distributed coordination strategy is designed for each pair of conflicting platoons approaching from different directions. For the scheduling purpose, an optimization problem subject to the constraint of allowable arrival time is formulated to guarantee collision avoidance between two conflicted vehicular platoons approaching the intersection. Specifically, in order to comprehensively consider traffic efficiency and fuel economy, a weighted performance index is introduced to achieve combined-objective optimization. PMP and phase-plane method are used to analyze the detailed optimal control sequences under various traffic scenarios. The simulation results conclusively show the effectiveness of the proposed scheme.

The rest of this paper is organized as follows. In Section 2, the problem statement in the paper is defined. In Section 3, a vehicular platoon controller design procedure is presented to deal with the tracking problem of CAVs, and the solution of the optimization trajectory control problem by PMP method and phase-plane method is given. The simulation results are presented in Section 4. Section 5 concludes this study.

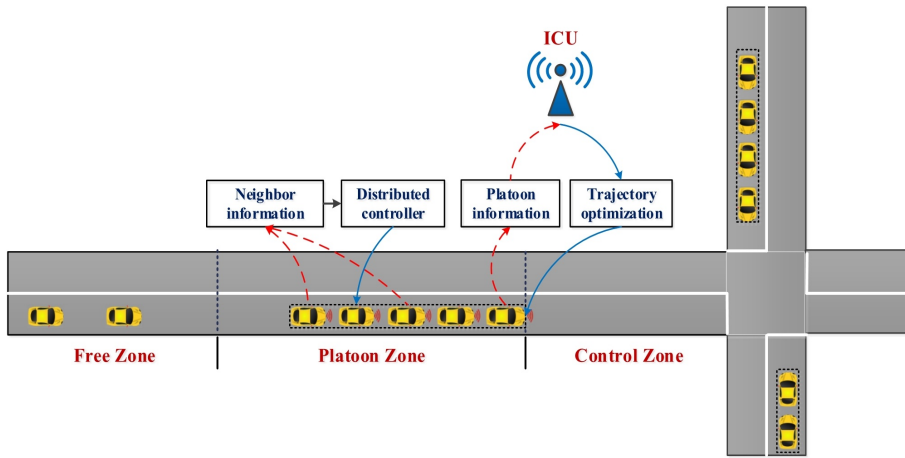


**Figure 1.** Scenario of intersection collaboration at a typical non-signalized intersection. Each approaching lane is divided into the free zone, the platoon zone, and the control zone. CAVs in the platoon zone and control zone exchange information with neighbor vehicles in the same platoon. The intersection coordination unit (ICU) receives the platoon information when the leading vehicle enters the control zone. The vehicles surrounded by dotted lines make up a platoon.

## 2. Problem statement

We consider a non-signalized intersection, which contains vehicles, road segments and an intersection coordination unit (ICU). The ICU has functions of both communication and computation. Vehicles equipped with V2V device can exchange information and communicate with the ICU within a specific communication range via V2I device. As is shown in Figure 1, taking one approaching lane as an example, it is divided into three sections, i.e., the free zone, the platoon zone and the control zone. Individual behaviors, such as overtaking and lane-changing, are only allowed in the free zone. CAVs are expected to compose automated vehicular platoons when they enter the platoon zone and the control zone. When a vehicular platoon enters the control zone, the leading vehicle will interact with the ICU for coordination information. For developing a coordination framework of CAVs crossing a non-signalized intersection, some assumptions are made as follows:

- The control of lateral motions, such as lane changing, overtaking and turning, is not considered in this paper.
- Some problems introduced by the communication network, such as communication delays, packet dropouts and quantization errors, are not included in this paper.

To enable all CAVs to pass through the non-signalized intersection without collision, while optimizing the trajectory of each leading vehicle to balance fuel consumption and travel time, a framework is put forward. The framework mainly consists of two parts: the tracking control of CAVs operating in the platoon zone and the control zone, and the trajectory optimization of the leading vehicle in the control zone. In the platoon zone, a string of individual vehicles are commanded to form an automated platoon including one leading vehicle and other following vehicles. Each vehicle can exchange state information (position and velocity) with neighboring vehicles in real time. Once arriving at the con-

trol zone, the leading vehicle interacts with the ICU for instantaneous information by the following process:

- 1) When the leading vehicle of the (host) platoon enters the control zone, the information, e.g., the initial velocity of the leading vehicle and the number of vehicles in the platoon, is sent to the ICU immediately.
- 2) The ICU calculates the allowable minimum arrival time of the host leading vehicle for avoiding a collision according to the current status of the platoons on other approaching lanes, and then it transmits it to the host leading vehicle.
- 3) Then, the leading vehicle optimizes its trajectory based on the designed performance index, such as minimizing arriving time or minimizing fuel consumption, under the constraints of the allowable minimum arrival time.

Once the leading vehicle completes information exchanging with the ICU, the potential trajectory of the leading vehicle is determined. Such a framework can save network bandwidth since it avoids frequent communication between vehicles and ICU.

### 2.1. Model for vehicle longitudinal dynamics

Consider an independent string of CAVs composed of  $N+1$  vehicles running in the platoon zone or control zone as shown in Figure 2. For each vehicle, the longitudinal dynamics includes the engine, powertrain, brake system, aerodynamics drag, tire friction, rolling resistance and gravitational force. Define  $s_i$  and  $v_i$  as the distance to the intersection stop line and the velocity of the vehicle  $i$  ( $i = 0, 1, \dots, N$ ), respectively. According to [17, 19], the longitudinal dynamics of the vehicle  $i$  can be described by the following nonlinear differential equations

$$\begin{cases} \dot{s}_i = v_i \\ \dot{v}_i = \frac{1}{M_i} \left( \eta \frac{T_i(t)}{R_a} - M_i g \mu_f - C_A v_i^2 \right) \end{cases} \quad (2.1)$$

where  $M_i$  is the mass of vehicle  $i$ ,  $T_i(t)$  is the actual driving/braking torque,  $\eta$  is the mechanical efficiency of the powertrain,  $R_a$  is the tire radius,  $g$  is the gravity constant,  $\mu_f$  is the coefficient of rolling resistance, and  $C_A$  is the coefficient of aerodynamic drag. To facilitate the system analysis and controller design, the nonlinear model in (2.1) is converted into a linearized one by using the exact feedback linearization technique [17, 19]:

$$T_i(t) = \frac{R_a}{\eta} (C_A v_i^2 + M_i g \mu_f + M_i u_i) \quad (2.2)$$

where  $u_i$  is the desired control input. Then, substituting (2.2) into (2.1) leads to a second-order model of vehicle longitudinal dynamics as follows:

$$\begin{cases} \dot{s}_i = v_i \\ \dot{v}_i = u_i \end{cases} \quad i = 0, 1, \dots, N. \quad (2.3)$$

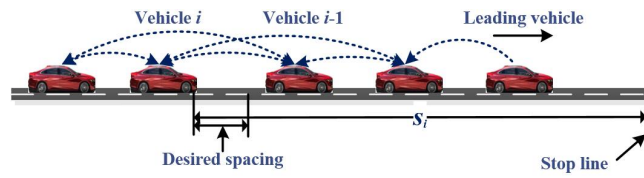


**Figure 2.** A vehicular platoon with two bidirectional predecessors following topology.

## 2.2. Distributed coordination for conflicting vehicular platoons

Formation of CAVs enables individual vehicles to cluster as a whole. Distributed coordination for vehicular platoons aims at scheduling each pair of conflicting platoons approaching from different directions to cross the intersection without collision. Conflict situations from different directions at a typical intersection can be classified into three types, including crossing, converging and non-conflicting, as shown in Figure 3. The red line and the blue line represent two vehicular platoons crossing the intersection, named as platoon  $I_1$  and platoon  $I_2$ , respectively. In this paper, the First Come First Served (FCFS) basis is adopted, where the platoon entering the control zone earlier has a higher priority to cross the intersection. It is assumed that platoon  $I_1$  enters control zone first, and the trajectory of the platoon  $I_1$  has been determined by its preceding conflicting platoon. To avoid a collision with the platoon  $I_1$ , the trajectory and arrival time of the platoon  $I_2$  need to be planned. To cope with different conflict situations at the intersection, four coordination modes are presented.

Mode I: This mode is applied to the “Crossing” situation (Figure 3(a)). The platoon  $I_2$  has to reach the stop line after the platoon  $I_1$  passes through the intersection. Here, we define  $\tau^*$  as predicted time from the moment the platoon  $I_2$  enters the control zone (the reference point to measure time) to the instant when the platoon  $I_1$  completely passes the center of the intersection. To be specific, for the coordinated platoon  $I_2$ ,  $\tau^*$  can be estimated as  $\tau^* = t_{I_1}^{act} + t_{I_1}^c + t_{I_1}^u$ , where  $t_{I_1}^{act}$  is the arrival time of the platoon  $I_1$ ,  $t_{I_1}^c$  is the cross time of the platoon  $I_1$  at the central area of the intersection, and  $t_{I_1}^u$  is the reserved clearance time. Thus, the platoon  $I_2$  reaches the intersection with arrival time  $t_f(I_2)$  satisfying  $t_f(I_2) \geq \tau^*$  for preventing collision.  $\tau^*$  is allowable minimum arrival time of the platoon  $I_2$ .

Mode II: This mode is suitable for the conflict situation of “Converging” (Figure 3(b)). To avoid collision of the two platoons, the arrival time of the platoon  $I_2$  must lag behind the time when the platoon  $I_1$  crosses the intersection. The calculation of  $\tau^*$  is same with Mode I. Particularly, in order to avoid rear-end collision between the tail vehicle of the platoon  $I_1$  and the leading vehicle of the platoon  $I_2$  after converging, the terminal velocities must be satisfied, i.e.,  $v_l^{I_2}(t_f) \leq v_l^{I_1}(t_f)$ , where  $v_l^{I_2}(t_f)$  and  $v_l^{I_1}(t_f)$  are the terminal velocities of the leading vehicle of the platoon  $I_2$  and the platoon  $I_1$ , respectively, when they reach the stop line.

Mode III: This mode adapts for the situation that two non-conflicting platoons can cross the intersection at the same time, e.g., shown in Figure 3(c). When the platoon  $I_2$  enters the control zone, the remaining time for the platoon  $I_1$  to reach and cross the intersection is defined as “conflict-free time” of the platoon  $I_2$ . To prevent collision with the subsequent coming platoons conflicting with the platoon  $I_1$ , the trajectory of the platoon  $I_2$  needs to be planned to guarantee crossing the intersection completely within the conflict-free time.

Mode IV: This mode applies for the other case different from Mode III. The platoon  $I_2$  cannot pass the intersection completely within the conflict-free time. The ICU will calculate the maximum number of vehicles in the platoon  $I_2$  able to cross the intersection during the conflict-free time and instruct the platoon  $I_2$  to split into two new platoons by V2I communication. The former one will continue to pass through the intersection first, while the later one will be coordinated with its conflicting platoon from other directions. The specific description will be shown in the simulation example.

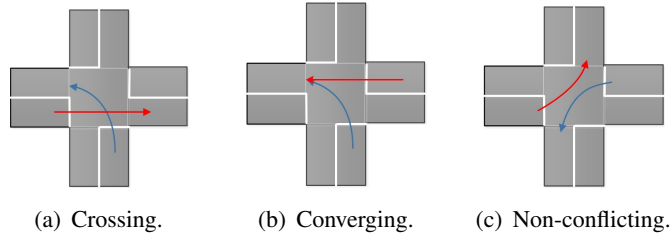


**Figure 3.** Conflict situations.

The general flowchart of the coordination strategy is shown in Figure 4. The results of distributed coordination for conflicted platoons give a range of allowable arrival time of the later approaching platoon for collision avoidance. The allowable arrival time is a key constraint on the trajectory optimization of the leading vehicle.

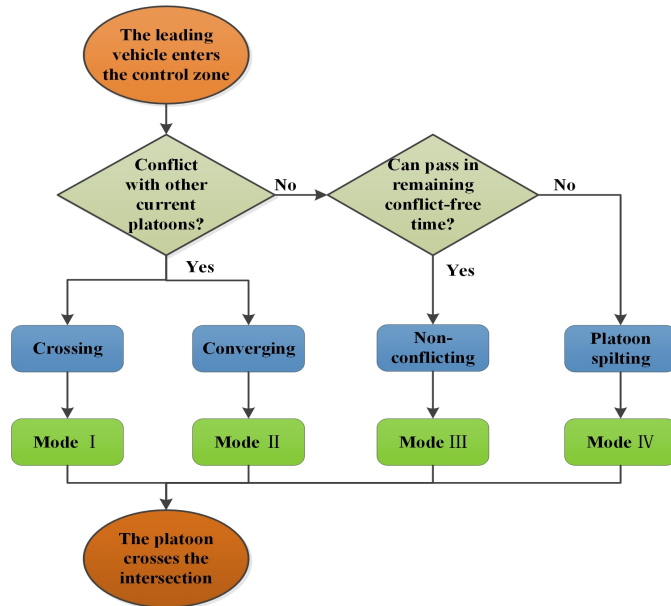


**Figure 4.** The general flowchart of the coordination strategy.

### 2.3. Optimization model for the leading vehicle

Once the coordination strategy mode is determined, the coordination problem is converted into a trajectory optimization problem of the leading vehicle. Considering the fuel consumption and travel

time simultaneously, the optimization problem of the leading vehicle can be formulated as follows:

$$(u_0^*, t_f^*) = \arg \min_{u_0} J(u_0, t_f) \quad (2.4)$$

subject to

$$J(u_0, t_f) = \int_0^{t_f} (\sigma + |u_0|) dt \quad (2.5)$$

$$\dot{x}_0(t) = \begin{bmatrix} \dot{s}_0(t) \\ \dot{v}_0(t) \end{bmatrix} = \begin{bmatrix} v_0(t) \\ u_0(t) \end{bmatrix} \quad (2.6)$$

Considering the limitation of vehicle powertrain and travel comfort of the passengers, the acceleration of the leading vehicle is subjected to be piecewise continuous and bounded, i.e.,  $|u_0| \leq \omega$ , where  $\omega = \max\{|a_{max}|, |a_{min}|\}$ . The constraints of velocity and acceleration are

$$a_{min} \leq u_0(t) \leq a_{max}, \quad (2.7)$$

$$v_{min} < v_0(t) \leq v_{max}. \quad (2.8)$$

The initial conditions are

$$\begin{cases} s_0(0) = -L, \\ v_0(0) = V_0. \end{cases} \quad (2.9)$$

The terminal state conditions are

$$\begin{cases} s_0(t_f) = 0, \\ v_0(t_f) = V_{tf}. \end{cases} \quad (2.10)$$

The constraint of terminal time satisfies

$$t_f \geq \tau^* \quad (2.11)$$

In the formulation,  $\sigma$  is a pre-set constant and serves as the weight factor to balance the travel time and fuel consumption;  $a_{min}$  and  $a_{max}$  represent the allowable maximum deceleration and acceleration, respectively;  $v_{max}$  and  $v_{min}$  denote the specified maximum and minimum velocity, respectively;  $V_0$  is the initial velocity of the leading vehicle upon entering the control zone;  $V_{tf}$  is the terminal velocity of the leading vehicle when its front bumper reaches the stop line;  $L$  is the length of the control zone;  $t_f$  is the arrival time to reach the stop line;  $\tau^*$  is allowable minimum arrival time as introduced in the previous subsection.

From a fuel economy perspective, minimizing the accumulation of control inputs of all the vehicles generally results in the improvement of fuel efficiency. For the sake of traffic efficiency, minimizing the arrival time of the leading vehicle can improve traffic throughput. Thus, there is a trade-off between the two performances as shown in Eq (2.5). For instance, providing a higher weight to the travel time of the leading vehicle may obtain better performance on traffic throughput, while increasing fuel consumption of the host platoon. Therefore, the weight factor  $\sigma$  should be adjusted according to actual traffic demand.

**Remark 1.** The simplified two-order model (2.6) is used for trajectory planning purpose. The facilities are twofold: 1) The double-integral model is easy to solve with optimization problems in various conditions which have been commonly used in relevant literature, e.g., [28]. These obtained optimized control inputs then can serve as reference input signals of lower-level vehicle controllers. 2) The formulated time-fuel optimization control problem has analytic solutions for the double integral model, and PMP can be applied to solve this problem [29].

**Remark 2.** We formulate the trajectory optimization problem of the leading vehicle instead of the whole vehicular platoon. It is empirically believed that trajectory optimization of the leading vehicle can promote the optimization of the whole vehicular platoon to some extent, since the following vehicles track the trajectory of their leading vehicle due to the effective tracking control algorithm [30]. This simplification can reduce the complexity of solving the optimization problem.

#### 2.4. Objective

The objective of this paper: let CAVs cross the non-signalized intersection safely and efficiently. To realize this objective, we jointly design the distributed cooperative tracking control and optimize the trajectory of the leading vehicle as follows.

- 1) Tracking control: We design the distributed controllers for all the following vehicles in the platoon zone and the control zone to track the trajectory of their leading vehicle, while maintaining a desired inter-vehicle gap, i.e.,

$$\begin{cases} s_i(t) \rightarrow s_{i-1}(t) - d_{i,i-1} - l_{i-1} \\ v_i(t) \rightarrow v_0(t) \end{cases} \quad i = 1, \dots, N,$$

where  $d_{i,i-1}$  is the desired gap between vehicle  $i$  and  $i - 1$ , and  $l_{i-1}$  is the length of vehicle  $i - 1$ .

- 2) Trajectory planning optimization: By planning the trajectory of the leading vehicles with the help of the ICU, all the vehicular platoons pass through the intersection without stopping halfway or collision with platoons from other directions, and travel time and fuel consumption of the leading vehicle are optimized comprehensively. To be specific, the optimal control law is designed to solve the optimization problem (2.4).

### 3. Solution methods

In this section, a distributed vehicular tracking controller design method and the solution method for trajectory optimization of the leading vehicle are proposed to achieve the objectives outlined in the previous section.

#### 3.1. Distributed vehicular tracking control

Automated vehicles are regulated to form a vehicular platoon upon entering the platoon zone and the control zone. Each following vehicle in the platoon intends to track the trajectory of the leading vehicle with a desired gap until crossing the intersection. The model in (2.3) can be written in the following form:

$$\dot{x}_i = Ax_i + Bu_i \quad i = 0, 1, \dots, N \quad (3.1)$$

where  $x_i = [s_i(t) \ v_i(t)]^T$ ,  $A = \begin{bmatrix} 0 & 1 \\ 0 & 0 \end{bmatrix}$ ,  $B = \begin{bmatrix} 0 & 1 \end{bmatrix}^T$ .

To meet the tracking objective for each following vehicle, the new auxiliary variables of errors  $\tilde{s}_i$  and  $\tilde{v}_i$  are defined by

$$\begin{cases} \tilde{s}_i(t) = s_i(t) - s_0(t) + \sum_{j=1}^i (d_{j,j-1} + l_{j-1}) \\ \tilde{v}_i(t) = v_i(t) - v_0(t) \end{cases} \quad (3.2)$$

where  $d_{j,j-1}$  is the desired gap between vehicle  $j$  and  $j-1$ , and  $l_{j-1}$  is the length of vehicle  $j-1$ .

Define the tracking error state as  $z_i(t) = [\tilde{s}_i(t) \ \tilde{v}_i(t)]^T$ . Then, substituting Eq (3.2) into the vehicular dynamics (3.1) can yield the following error system:

$$\dot{z}_i = Az_i(t) + Bu_i - Bu_0, \quad i = 1, \dots, N. \quad (3.3)$$

Note that here we release the restriction of zero input of the leading vehicle, which is different from the general hypothesis in the literature [21, 31]. Such a hypothesis is unpractical since the acceleration of the leading vehicle will be changed with the actual traffic conditions. The two bidirectional predecessors following topology is adopted for information transmission between vehicles as shown in Figure 2. According to the state information of the neighbor vehicles received by V2V communication, the tracking control law of the following vehicle  $i$  is proposed as

$$u_i(t) = \theta_1 K \sum_{j \in \Omega} (z_i(t) - z_j(t)) + \theta_2 \text{sign}\left(K \sum_{j \in \Omega} (z_i(t) - z_j(t))\right) \quad (3.4)$$

where  $K = [k_s \ k_v]$ ,  $k_s$  and  $k_v$  are position and velocity feedback gains to be designed, respectively.  $\Omega = \{i-2, i-1, i+1, i+2\}$ .  $\theta_1$  and  $\theta_2$  are coupling strengths. Substituting the control law (3.4) into the error system (3.3), the closed-loop dynamics of the errors becomes

$$\dot{z}_i(t) = AZ_i(t) + \theta_1 BK \sum_{j \in \Omega} (z_i(t) - z_j(t)) + \theta_2 \text{sign}\left(K \sum_{j \in \Omega} (z_i(t) - z_j(t))\right) - Bu_0(t) \quad (3.5)$$

Define the overall state errors incorporating all the following vehicles as  $Z = [z_1^T, z_2^T, \dots, z_N^T]^T \in R^{2N \times 1}$ , and it follows that

$$\begin{aligned} \dot{Z}(t) &= (I_N \otimes A + \theta_1 (L_N \otimes BK)) Z(t) + \theta_2 (I_N \otimes B) \\ &\quad \text{sign}((L_N \otimes K)Z(t)) - (\mathbf{1} \otimes B)u_0(t) \end{aligned} \quad (3.6)$$

where  $\otimes$  denotes the matrix Kronecker product, and  $L_N \in R^{N \times N}$  is the Laplacian matrix for all the following vehicles, characterizing the communication relationships among them,

$$L_N = \begin{bmatrix} 3 & -1 & -1 & & & \\ -1 & 4 & -1 & -1 & & \\ -1 & \ddots & \ddots & \ddots & \ddots & \\ & -1 & -1 & 4 & -1 & -1 \\ & & -1 & -1 & 3 & -1 \\ & & & -1 & -1 & 2 \end{bmatrix}$$

Clearly, the distributed vehicular platoon tracking problem (3.2) will be solved if the system (3.6) is stabilized. To obtain the result of the platoon controller design, the following lemma is introduced.

**Lemma 1.** [32] *Given a matrix pair  $(A, B)$ , where  $A \in R^{n \times n}$ ,  $B \in R^{n \times m}$ , and  $m \leq n$ , there exists a positive definite matrix  $P \in R^{n \times n}$  such that*

$$AP + PA^T - 2BB^T + 2\alpha P < 0$$

*holds for any arbitrary  $\alpha > 0$ , if  $(A, B)$  is controllable.*

**Theorem 1.** *The distributed platoon tracking problem (3.2) for the vehicular system (2.3) can be solved by the control law (3.6) if there exist a positive scalar  $\alpha$  and a positive definite matrix  $P$  such that*

$$AP + PA^T - 2BB^T + 2\alpha P < 0. \quad (3.7)$$

*Then, the controller gain is given by  $K = -B^T P^{-1}$ , and the coupling strengths of the controller satisfy  $\theta_1 \geq 1/\lambda_{\min}(L_N)$  and  $\theta_2 \geq \omega$ ,  $\omega = \max\{|a_{\max}|, |a_{\min}|\}$ , while the spacing errors converge to zero exponentially faster than  $\exp(-\alpha t)$ .*

The proof for Theorem 1 is attached in Appendix A.

### 3.2. Trajectory optimization for leading vehicle

The optimization problem (2.4) subject to (2.5)–(2.10) can be solved by applying PMP preliminary, and the final optimal analytic solution is further obtained by the phase-plane method.

First, we introduce the Hamiltonian function

$$H(t) = \sigma + |u_0(t)| + \gamma_1(t)v_0(t) + \gamma_2(t)u_0(t), \quad (3.8)$$

where  $\gamma_1(t)$  and  $\gamma_2(t)$  are the co-state variables related to the state variables  $s_0(t)$  and  $v_0(t)$ , respectively.

To minimize the Hamiltonian function, the optimal control  $u_0^*(t)$  should fulfill the following condition:

$$\begin{aligned} & \sigma + |u_0^*(t)| + \gamma_1(t)v_0(t) + \gamma_2(t)u_0^*(t) \\ & \leq \sigma + |u_0(t)| + \gamma_1(t)v_0(t) + \gamma_2(t)u_0(t). \end{aligned} \quad (3.9)$$

Thus, the optimal control can be written as

$$u_0^*(t) = \begin{cases} a_{\max}, & \gamma_2(t) < 1 \\ 0, & -1 < \gamma_2(t) < 1 \\ a_{\min}, & \gamma_2(t) > 1 \\ [a_{\min}, 0], & \gamma_2(t) = 1 \\ [0, a_{\max}], & \gamma_2(t) = -1. \end{cases} \quad (3.10)$$

The co-state equations are

$$\dot{\gamma}_1(t) = -\frac{\partial H}{\partial s_0} = 0 \quad (3.11)$$

$$\dot{\gamma}_2(t) = -\frac{\partial H}{\partial v_0} = -\gamma_1(t). \quad (3.12)$$

Suppose that initial co-states are  $\gamma_1(0)$  and  $\gamma_2(0)$ , and then the co-states can be solved as

$$\gamma_1(t) = \gamma_1(0) = c \quad (3.13)$$

$$\gamma_2(t) = \gamma_2(0) - \gamma_1(0)t \quad (3.14)$$

where  $c$  is a constant. Hamiltonian function  $H$  along the optimal trajectory satisfies

$$H^*(t) = \sigma + |u_0^*| + \gamma_1(t)v_0^* + \gamma_2(t)u_0^* = 0 \quad (3.15)$$

where  $\sigma > 0$  and  $|u_0^*| \geq 0$ . Notice that in (3.15),  $\gamma_1(t)$  and  $\gamma_2(t)$  are not equal to zero simultaneously, otherwise  $H^*(t) > 0$ . Similarly, note that in (3.13) and (3.14), neither  $\gamma_1(0)$  nor  $\gamma_2(0)$  can be equal to zero at the same time. Thus, Eq (3.14) is monotonic, and there is no singular control case.

According to the above analysis, nine control sequences can be recognized based on the initial and the terminal values of  $\gamma_2(t)$ . The nine control sequences are expressed as:  $\{a_{min}\}$ ,  $\{0\}$ ,  $\{a_{max}\}$ ,  $\{0, a_{min}\}$ ,  $\{a_{min}, 0\}$ ,  $\{0, a_{max}\}$ ,  $\{a_{max}, 0\}$ ,  $\{a_{min}, 0, a_{max}\}$ ,  $\{a_{max}, 0, a_{min}\}$ .

Notice that the arrival time  $t_f$  is strictly constrained by the inequality (Eq 2.11), which means the analytic solutions of optimal problem (2.4) may not be obtained using PMP merely. Thus, the phase-plane method is presented to assist in obtaining the optimal control solutions. In order to ensure having enough distance to adjust vehicle velocity, it requires that  $L$  is long enough for a vehicle to accelerate from the minimum velocity to the limited maximum with the maximum acceleration and then to decelerate from the maximum velocity to its minimum with the maximum deceleration. We assume that the length of the control zone satisfies

$$L \geq \frac{v_{max}^2 - v_{min}^2}{2a_{max}} + \frac{v_{min}^2 - v_{max}^2}{2a_{min}} \quad (3.16)$$

Depending on different initial velocity  $V_0$ , the terminal velocity  $V_{tf}$  and the coordinated allowable minimum arrival time  $\tau^*$ , various cases and their corresponding optimal control sequences are analyzed as follows:

1) **Case 1:**  $V_0 = V_{tf}$

$T_a$  and  $T_c^{fea,u}$  denote the arrival time shown in Figure 5(a) and the upper boundary of the arrival time shown in Figure 5(c), respectively, when a feasible solution exists.

a) Case 1.1:  $\tau^* \leq T_a$

In this case, the leading vehicle only needs to maintain the constant velocity with control sequence  $\{0\}$  to the stop line without acceleration or deceleration.  $T_a$  can be simply obtained by  $T_a = L/V_0$ . If  $\tau^*$  is absolutely smaller than  $T_a$ , the control sequence may be a three-segment sequence  $\{a_{max}, 0, a_{min}\}$  shown in Figure 5(b) for a shorter arrival time which depends on the values of  $\tau^*$  and the weight  $\sigma$ .

b) Case 1.2:  $T_a < \tau^* \leq T_c^{fea,u}$

In this case, the leading vehicle has to decelerate first, then maintains a constant velocity, and finally accelerates to fulfill the requirements of arrival time and terminal velocity with the control sequence  $\{a_{min}, 0, a_{max}\}$  shown in Figure 5(c).

c) Case 1.3:  $\tau^* > T_c^{fea,u}$

No feasible solution can be found in this case. In other words, it is not possible to move the leading vehicle from initial state to final state over time  $\tau^*$  unless the vehicle stops in the middle, which is not allowed in this paper.

2) **Case 2:**  $V_0 > V_{tf}$

$T_e$  and  $T_g$  denote the arrival time shown in Figure 5(e) and Figure 5(g), respectively, and  $T_h^{fea,u}$  is defined as the upper boundary of arrival time shown in Figure 5(h) when a feasible solution exists.

a) Case 2.1:  $\tau^* \leq T_e$

$T_e$  can be easily solved by one equation set containing a constant velocity segment and a deceleration segment. In this case, either the three-segment control sequence  $\{a_{max}, 0, a_{min}\}$  shown in Figure 5(d) or the two-segment control sequence  $\{0, a_{min}\}$  shown in Figure 5(e) may be the optimal feasible solution, which also depends on the values of  $\tau^*$  and  $\sigma$ .

b) Case 2.2:  $T_e < \tau^* \leq T_g$

In this case, two-segment control sequence  $\{a_{min}, 0\}$  shown in Figure 5(g) or three-segment control sequence  $\{a_{min}, 0, a_{min}\}$  shown in Figure 5(f) may be the optimal feasible solution depending on the values of  $\tau^*$  and  $\sigma$ . Notice that  $\{a_{min}, 0, a_{min}\}$  does not belong to any of the nine scenarios in ordinary control due to the constraint of the arrival time and the selection of  $\sigma$ .

c) Case 2.3:  $T_g < \tau^* \leq T_h^{fea,u}$

This case is similar to Case 1.2, and the control sequence  $\{a_{min}, 0, a_{max}\}$  is supposed to be adopted.

d) Case 2.4:  $\tau^* > T_h^{fea,u}$

No feasible solution can be found in this case. The reason is similar to Case 1.3.

3) **Case 3:**  $V_0 < V_{tf}$

In this case, the scenario classifications are analogous with **Case 2**, and we integrally show them in Figure 5(i). The detailed discussion is omitted here.

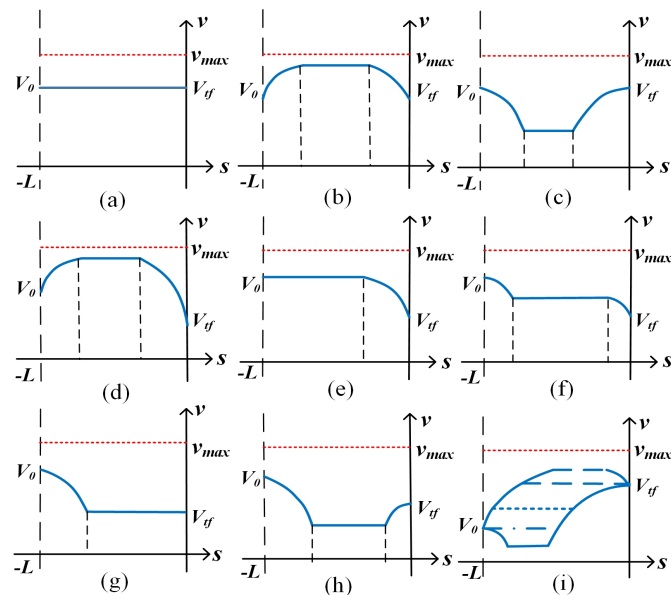


**Figure 5.** Phase-plane diagram under different control sequences.

All possible optimal control sequences defined above depend on the initial velocity  $V_0$ , the terminal velocity  $V_{tf}$ , the allowable minimum arrival time  $\tau^*$  and the selected weight  $\sigma$ . The optimal control

sequences under different conditions are displayed in Table 1. Then, the algebraic equations of the system for each control sequence can be constructed, where the switching time can be solved. Taking the complex case  $\{a_{min}, 0, a_{max}\}$  in Figure 5(h) as an example, the development of the algebraic equations is found in Appendix B. Other cases can be solved in a similar way.

**Table 1.** Optimal control sequences under different conditions.

Case	$V_0 = V_{lf}$	$\tau^* \leq T_a$	$T_a < \tau^* \leq T_c^{fea,u}$	$\tau^* > T_c^{fea,u}$	$V_0 < V_{lf}$	$\tau^* \leq T_e$	$T_e < \tau^* \leq T_g$	$T_g < \tau^* \leq T_h^{fea,u}$	$\tau^* > T_h^{fea,u}$
Arrival time	$T_a$ or $T_b$	$T_c$	$XX$		$T_d$ or $T_e$	$T_g$ or $T_f$	$T_h$	$XX$	
Optimal control sequence	$\{0\}$ or $\{a_{max}, 0, a_{min}\}$	$\{a_{min}, 0, a_{max}\}$		No feasible solution	$\{a_{max}, 0, a_{min}\}$ or $\{0, a_{min}\}$	$\{a_{min}, 0\}$ or $\{a_{min}, 0, a_{min}\}$	$\{a_{min}, 0, a_{max}\}$		No feasible solution
Switching times	0 or 2	2	$XX$	2 or 1	1 or 2	2	$XX$		

## 4. Simulation results

In this section, simulations are conducted to evaluate the performance of the presented scheme for collaborative intersection control. In the first scenario, we test the tracking performance of a vehicular platoon consisting of nine vehicles. Then, the effectiveness of the proposed intersection collaboration strategy is evaluated in the second scenario, in which 24 vehicles are initially distributed in three directions approaching the intersection. Finally, we analyze the influence of different weights on fuel consumption and travel time in the second scenario.

### 4.1. Scenario of platoon tracking

A numerical case is given to verify the proposed platoon control method. In this case, we consider a string of CAVs including nine vehicles (one leader and eight followers) moving on an approaching lane. The initial states of each vehicle are set as  $x_0(0) = [-400 \ 13]^T$ ,  $x_1(0) = [-412 \ 13]^T$ ,  $x_2(0) = [-433 \ 10]^T$ ,  $x_3(0) = [-448 \ 13]^T$ ,  $x_4(0) = [-459 \ 12]^T$ ,  $x_5(0) = [-473 \ 13]^T$ ,  $x_6(0) = [-491 \ 14]^T$ ,  $x_7(0) = [-502 \ 12]^T$ ,  $x_8(0) = [-521 \ 14]^T$ , respectively. The desired inter-vehicle distance is selected as 10 m, and the length of each vehicle is 5 m. The communication topology is adopted as shown in Figure 2, and thus  $\lambda_{min}(L_N) = 0.1383$  can be acquired. The upper bound of the absolute value of the acceleration is regulated as  $2 \text{ m/s}^2$ , and  $\omega = 2$  is chosen. Since the coupling strengths  $\theta_1$  and  $\theta_2$  are constrained by  $\lambda_{min}(L_N)$  and  $\omega$ , we select  $\theta_1 = 7.5$ ,  $\theta_2 = 2$  and  $\alpha = 0.1$ . According to Theorem 1, the tracking controller gain matrix  $K = [-1.2970 \ -2.8952]$  can be obtained by using the "Yalmip" tool to solve the linear matrix inequality in (Eq 3.7). The vehicular platoon starts at  $t = 0$  s, and the total simulation time is 30 s. The velocity trajectory of the leading vehicle is set as

$$v_0(t) = \begin{cases} 13 + 1t, & t \in [0, 5s) \\ 18, & t \in [5s, 11s) \\ 18 - 2t, & t \in [11s, 15s) \\ 10, & t \in [15s, 30s]. \end{cases} \quad (4.1)$$

In the example, the velocity of the leading vehicle changes with the prescribed profile. Figure 6 shows that the following vehicles can track the velocity of the leading vehicle with the desired inter-vehicle gap. Figure 7 shows variation of spacing error between each two successive vehicles. It can be seen that tracking errors occur at the initial time and the instants when the velocity of the leading

vehicle changes. The spacing errors converge to zero at around  $t = 10$  s and  $t = 20$  s, respectively. Thus, it is demonstrated that the proposed tracking controller design method can meet the tracking objective presented in this paper.

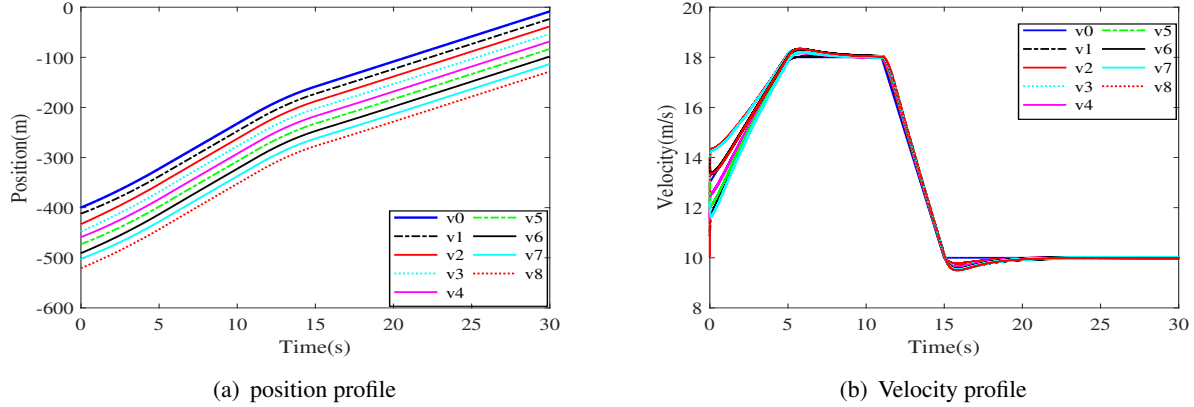


**Figure 6.** The trajectories of CAVs.

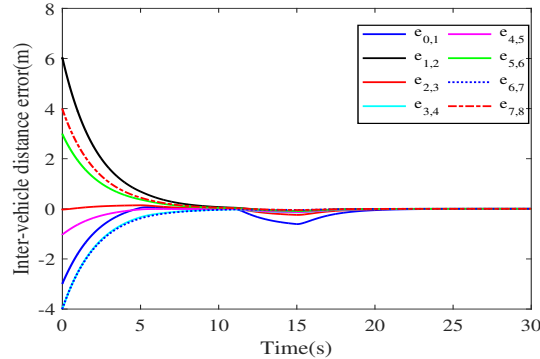


**Figure 7.** The inter-vehicle distance errors between two successive vehicles.

#### 4.2. Scenario of coordination

To illustrate the effectiveness of the proposed coordination strategy for CAVs through the non-signalized intersection without collision, another numerical example is given. A local traffic scenario shown in Figure 8 comprises 24 vehicles, which form three vehicular platoons, i.e., platoon A, platoon B and platoon C, approaching from the west, the south and the east, respectively. The leading vehicles of the three platoons are denoted as  $LV_A$ ,  $LV_B$  and  $LV_C$ , respectively. The effectiveness of tracking control of vehicles within a single platoon has been verified in the previous scenario. Here, we focus on the performance of the proposed coordination strategy for CAVs crossing the intersection without collision.

Figure 8 shows the initial positions and heading directions of the three platoons. The platoon A approaching from the west is going to turn left into the intersection and then heads north. The platoon B conflicts with the platoon A and moves toward the north from the south. The platoon C coming

from the east conflicts with the platoon  $B$  but not with the platoon  $A$ . The conflict types between each pairs of the three platoons, i.e.,  $(A, B)$ ,  $(B, C)$  and  $(C, A)$ , are converging, crossing and non-conflicting, respectively. The distances from the initial positions of  $LV_A$ ,  $LV_B$  and  $LV_C$  to the intersection are 270, 358, and 315 m, respectively. The initial velocities of the three leading vehicles are 15, 15 and 12 m/s, respectively. We regulate the three leading vehicles with the constant initial velocity before entering the control zone. The other related parameters of this example are shown in Table 2.

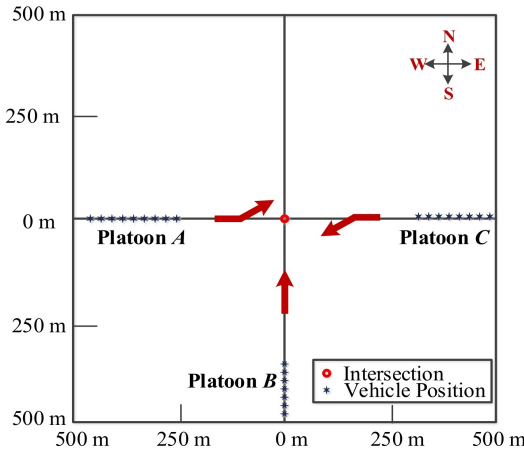


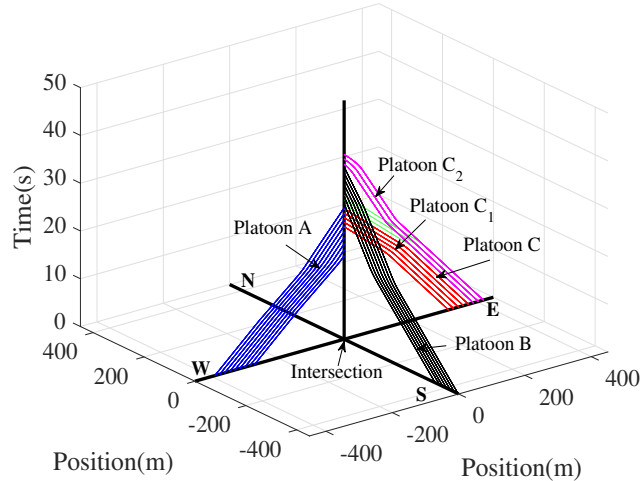
**Figure 8.** The initial position of vehicles in the coordination scenario.

**Table 2.** Default settings.

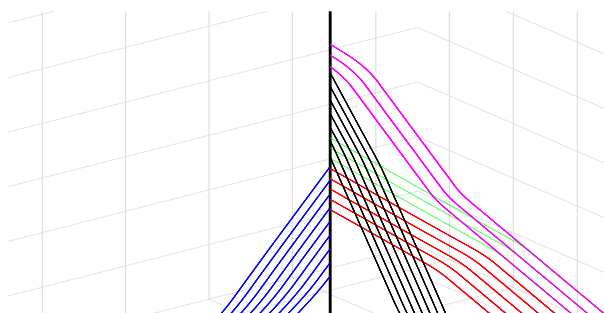
Parameter	Notation	Value
The length of the control zone	$L$	150 m
Desired vehicular gap	$d$	10 m
Vehicle length	$l$	5 m
Minimal speed	$v_{min}$	2 m/s
Maximal speed	$v_{max}$	18 m/s
Maximal deceleration	$a_{min}$	-2 m/s <sup>2</sup>
Maximal acceleration	$a_{max}$	2 m/s <sup>2</sup>
Weight factor	$\sigma$	5

We assume that the collaboration strategy Mode I is applied to coordinate the platoon  $A$  to prevent collision with its preceding conflicting platoon, the allowable minimum arrival time of  $LV_A$  is  $\tau_A^* = 8$  s, and the terminal velocity of  $LV_A$  is 12 m/s. The optimal control sequence of  $LV_A$  is obtained as  $\{a_{max}, 0, a_{min}\}$  depicted in the Figure 5(d). According to the predicted remaining time of the platoon  $A$  crossing the intersection,  $\tau_B^* = 15$  s is obtained for avoiding collision with the platoon  $A$ , and the terminal velocity of  $LV_B$  is set as 12 m/s for avoiding rear-end collision with the tail vehicle of the platoon  $A$  after converging. The collaboration strategy Mode II and the case shown in Figure 5(h) accord with the situation. The optimal control sequence of  $LV_B$  is obtained as  $\{a_{min}, 0, a_{max}\}$ . For the platoon  $C$ , the situation is more complicated. The platoon  $C$  intends to cross the intersection before the platoon  $A$  completely passes through the intersection for avoiding collision with the platoon  $B$ . However, the

remaining conflict-free time is not enough for the entire platoon  $C$  to pass through the intersection. The collaboration strategy Mode IV is used to address this problem. The platoon  $C$  is split into two new platoons, i.e., platoon  $C_1$  and platoon  $C_2$ . The first new platoon  $C_1$  crosses the intersection first, while the remaining platoon  $C_2$  passes after the platoon  $B$  crosses the intersection. The control sequence of  $LV_{C1}$  in the control zone is  $\{a_{max}, 0\}$  for passing through the intersection as soon as possible.  $\tau_{C_2}^* = 16.5$  s is obtained for preventing collision with the platoon  $B$ . The collaboration strategy Mode I and the case shown in Figure 5(b) are applied for the platoon  $C_2$ . Thus, the optimal control sequence of  $LV_{C2}$  is obtained as  $\{a_{min}, 0, a_{max}\}$ . The switching time of each optimal control sequence is obtained by solving the linear and nonlinear programming problems using the “fmincon” function of MATLAB.



(a) Position profiles



(b) Magnified position curves near the intersection

**Figure 9.** Position profiles of approaching vehicular platoons in the coordination scenario.

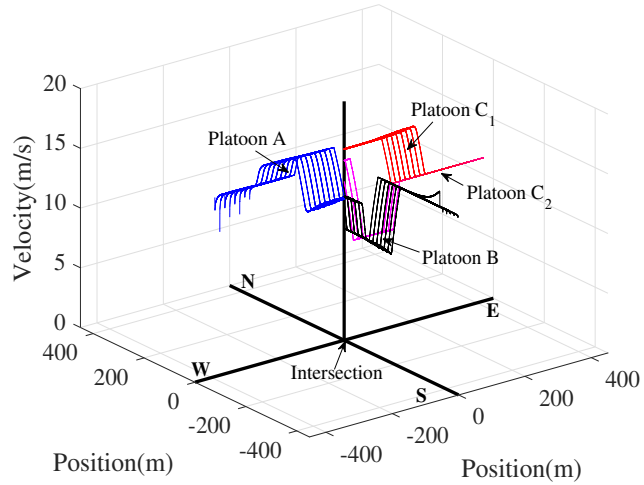


**Figure 10.** Velocity profiles of approaching vehicular platoons in the coordination scenario.

Figures 9 and 10 show the position and velocity profiles of the three platoons. It can be seen from Figure 9 that no collision occurs at the intersection. The platoon *B* reaches the intersection after the platoon *A* completely passes through the stop line. The platoon *C* cannot cross the intersection entirely, so it is split into two new platoons. The red lines represent the first new platoon *C*<sub>1</sub> that reaches the intersection as usual. The later platoon *C*<sub>2</sub> denoted by the magenta lines reaches the intersection after the platoon *B* completely passes through the stop line. The green lines represent the original trajectories of the platoon *C*<sub>2</sub>, which cause collision with the platoon *B* if it is not split from the original platoon *C*. It is worthy of noting that the confluence of the blue and red trajectories does not mean collision because of the non-conflicting relation between the platoon *A* and the platoon *C*. As is shown in Figure 10, all the vehicles keep constant velocity before entering the control zone. When each platoon enters the control zone, the vehicles within the platoon adjust their velocities in terms of the coordination results and the tracking control method. Specifically, the terminal velocities of the platoon *A* and the platoon *B* are identical, which prevent the rear-end collision between the two platoons. The simulation results show that the proposed intersection collaboration strategy can ensure that all the vehicles cross the intersection safely.

#### 4.3. Effect of weights on fuel cost and travel time

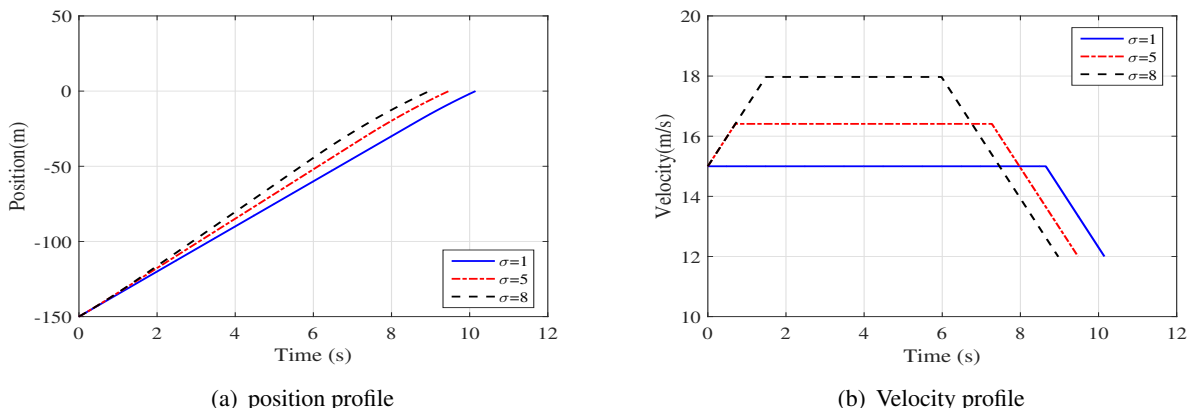
The combined cost function (2.5) involves a weight term to balance fuel cost and travel time of the leading vehicle of the host platoon. The selection of weight has an important influence on the trajectory of host platoon and even the results of coordination. A larger weight leads to a shorter travel time, but results in a larger fuel cost. An example of  $LV_A$  is used to clarify the effect under the different weights ( $\sigma = 1, 5, 8$ ). The timing starts when  $LV_A$  enters the control zone. Figure 11 shows the position and velocity trajectories of  $LV_A$  under the three different weights. As can be clearly seen from Figure 11(a),  $LV_A$  arrives at the intersection earlier with a larger weight. Correspondingly, different velocity profiles under the three weights are shown in Figure 11(b). When  $\sigma = 1$ , the fuel cost index plays a dominant role in the cost function, so  $LV_A$  keeps a constant velocity to avoid additional control inputs in the initial simulation period. As the weight increases, the index of travel time comes into play, and  $LV_A$

needs to accelerate to meet the requirement of a shorter travel time. When  $\sigma = 8$ ,  $LV_A$  accelerates to the maximum velocity, which leads to the shortest travel time. The contrasting results are displayed in Table 3.

To evaluate the fuel consumption of an entire platoon in the “Scenario of coordination,” we adopt the third-order polynomial model presented by Kamal et al. [33] to estimate the fuel consumption. The fuel consumption rate is formulated as a function of velocity, and acceleration,  $f_{rat} = f_{cru} + f_{acc}$ , where  $f_{cru} = p_0 + p_1v + p_2v^2 + p_3v^3$  denotes the fuel consumption rate at constant velocity, and  $f_{acc} = (q_0 + q_1v + q_2v^2)\dot{v}$  represents the extra fuel consumption due to acceleration. We set  $f_{acc}$  to zero when the vehicle does not accelerate ( $\dot{v} \leq 0$ ). The calibrated coefficients of the fuel consumption rate are  $p_0 = 0.1569$ ,  $p_1 = 2.45 \times 10^{-2}$ ,  $p_2 = -7.415 \times 10^{-4}$ ,  $p_3 = 5.975 \times 10^{-5}$ ,  $q_0 = 0.072$ ,  $q_1 = 9.681 \times 10^{-2}$  and  $q_2 = 1.075 \times 10^{-3}$ .

Figure 12 shows the comparison of the cumulative fuel consumptions of the platoon A under the different weights. The fuel consumption of all the vehicles in the platoon A is calculated under different weights within 30 s simulation time. During the period  $t = 0$ –8 s, the fuel consumption is the same under the three weights since the platoon has not entered the control zone and moves with the constant velocity. When  $t > 8$  s, after the platoon enters the control zone, the cumulative fuel consumption with a larger weight exceeds that with a smaller one. Figure 13 shows the instantaneous fuel consumption of the 5th vehicle in the platoon A under the three different weights. It is noticed that the values of instantaneous fuel consumption with the larger weight exceed that with the smaller weight during  $t = 8$ –10 s.

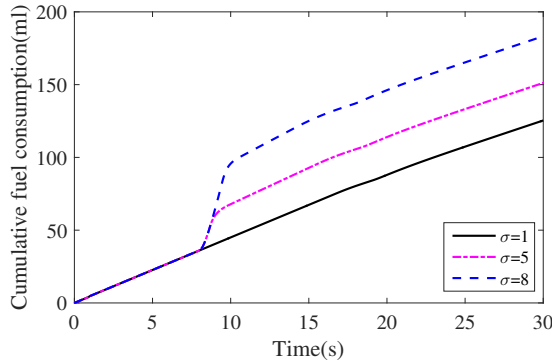
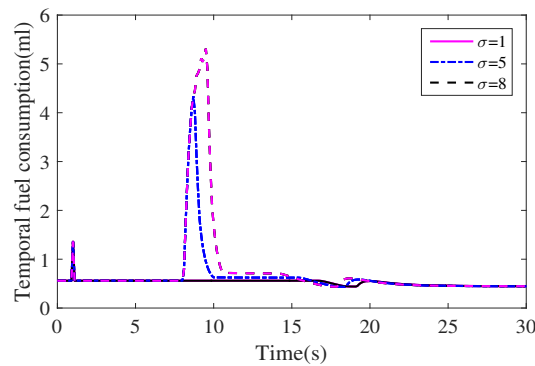
The above analysis indicates the influence of the weight on final trajectory of the platoon. In fact, the choice of weights may also have an impact on the results of the coordination among different platoons. For instance, considering the relation between the platoon A and the platoon C in the previous subsection “Scenario of coordination,” when we select  $\sigma = 1$ , the platoon A will arrive at the intersection later. Meanwhile the original platoon C could have more remaining time to allow one more vehicle to pass through the intersection in this case, i.e., six vehicles in the platoon  $C_1$ . Instead, if the weight  $\sigma = 8$  is chosen, one less vehicle in the platoon C can cross the intersection first, i.e., four vehicles in the platoon  $C_1$ . Therefore, how to choose the weight is supposed to refer to the actual traffic situation.



**Figure 11.** The trajectories of the leading vehicle of the platoon A in the control zone under different weights.

**Table 3.** Comparisons of fuel cost and travel time under different weights.

Weight $\sigma$	Fuel Cost	Travel Time (s)	Cost Function Value
1	3.0	10.2	13.2
5	5.8	9.5	53.2
8	9.0	8.9	80.7

**Figure 12.** Cumulative fuel consumption of the platoon A under different weights.**Figure 13.** Instantaneous fuel consumption of the 5th vehicle in the platoon A under different weights.

## 5. Conclusions

In this paper, we developed a cooperative intersection control scheme for CAVs. In order to coordinate CAVs through the non-signalized intersection, a platoon-based coordination framework was proposed. In this framework, each vehicular platoon was taken as a whole to be coordinated with other approaching platoons from different directions. First, to form automated vehicular platoons, a tracking control algorithm was proposed to drive all following vehicles to track the velocity of their leading vehicle with a desired spacing between adjacent vehicles. Then, a distributed coordination strategy was designed to schedule the arrival time of the leading vehicles approaching from different

directions. Specifically, considering the trade-off of traffic efficiency and fuel economy, a combined-objective optimal control problem of the leading vehicle was formulated under the constraint of the allowable minimum arrival time. PMP and phase plane analysis were applied to obtain optimal control sequences in diverse scenarios. Finally, simulation results showed the effectiveness of the proposed scheme.

Our future research work will consider communication issues in a CAV-based collaborative intersection control system such as transmission delay, data dropout and quantization. In addition, combined with the proposed method of the paper, how to develop an efficient vehicle coordination scheduling strategy at non-signalized intersections will be studied further.

## Acknowledgments

Jian Gong and Yuan Zhao contributed equally to this work. This work was supported by the National Natural Science Foundation of China under Grant 61833005, the Dalian Innovative Support Scheme for High-level Talents under Grant 2019RQ027, the Natural Science Foundation of Tianjin under Grant 20JCQNJC00390 and the Graduate Scientific Research Innovation Project of Tianjin under Grant 2021YJSO2S31.

## Conflict of interest

The authors declare there is no conflict of interest.

## References

1. B. Jeremy, T. Pete, K. Alan, B. Laurie, Y. George, E. Petros, et al., Traffic safety basic facts 2012: junctions, 2013. Available from: <https://roderic.uv.es/handle/10550/30218>.
2. NHTSA, Fatality Analysis Reporting System (FARS). Available from: <http://www.nhtsa.gov/FARS>.
3. P. B. Hunt, D. I. Robertson, R. D. Bretherton, R. I. Winton, SCOOT-a traffic responsive method of coordinating signals, 1981. Available from: <https://trid.trb.org/view/179439>.
4. A. G. Sims, K. W. Dobinson, The Sydney coordinated adaptive traffic (SCAT) system philosophy and benefits, *IEEE Trans. Veh. Technol.*, **29** (1980), 130–137. <https://doi.org/10.1109/T-VT.1980.23833>
5. S. C. Wong, W. T. Wong, C. M. Leung, C. O. Tong, Group-based optimization of a time-dependent TRANSYT traffic model for area traffic control, *Abbreviation Title Transp. Res. Part B Methodol.*, **36** (2002), 291–312. [https://doi.org/10.1016/S0191-2615\(01\)00004-2](https://doi.org/10.1016/S0191-2615(01)00004-2)
6. L. Chen, C. Englund, Cooperative intersection management: a survey, *IEEE Trans. Intell. Transp. Syst.*, **17** (2015), 570–586. <https://doi.org/10.1109/TITS.2015.2471812>
7. S. El-Tantawy, B. Abdulhai, H. Abdelgawad, Multiagent reinforcement learning for integrated network of adaptive traffic signal controllers (MARLIN-ATSC): methodology and large-scale application on downtown Toronto, *IEEE Trans. Intell. Transp. Syst.*, **14** (2013), 1140–1150. <https://doi.org/10.1109/TITS.2013.2255286>

8. A. Zaidi, B. Kulcsár, H. Wymeersch, Back-pressure traffic signal control with fixed and adaptive routing for urban vehicular networks, *IEEE Trans. Intell. Transp. Syst.*, **17** (2016), 2134–2143. <https://doi.org/10.1109/TITS.2016.2521424>
9. K. Dresner, P. Stone, Multiagent traffic management: a reservation-based intersection control mechanism, in *Proceedings of the Third International Joint Conference on Autonomous Agents and Multiagent Systems*, (2005), 471–477. <https://doi.org/10.1145/1082473.1082545>
10. K. Dresner, P. Stone, A multiagent approach to autonomous intersection management, *J. Artif. Intell. Res.*, **31** (2008), 591–656. <https://doi.org/10.1613/jair.2502>
11. M. Ahmane, A. Abbas-Turki, F. Perronnet, J. Wu, A. E. Moudni, J. Buisson, et al., Modeling and controlling an isolated urban intersection based on cooperative vehicles, *Transp. Res. Part C Emerging Technol.*, **28** (2013), 44–62. <https://doi.org/10.1016/j.trc.2012.11.004>
12. L. Li, F. Wang, Cooperative driving at blind crossings using intervehicle communication, *IEEE Trans. Veh. Technol.*, **55** (2006), 1712–1724. <https://doi.org/10.1109/TVT.2006.878730>
13. J. Lee, B. Park, Development and evaluation of a cooperative vehicle intersection control algorithm under the connected vehicles environment, *IEEE Trans. Intell. Transp. Syst.*, **13** (2012), 81–90. <https://doi.org/10.1109/TITS.2011.2178836>
14. M. A. S. Kamal, J. Imura, T. Hayakawa, A. Ohata, K. Aihara, A vehicle-intersection coordination scheme for smooth flows of traffic without using traffic lights, *IEEE Trans. Intell. Transp. Syst.*, **16** (2014), 1136–1147. <https://doi.org/10.1109/TITS.2014.2354380>
15. P. Dai, K. Liu, Q. Zhuge, E. H. Sha, V. C. S. Lee, S. H. Son, Quality-of-experience-oriented autonomous intersection control in vehicular networks, *IEEE Trans. Intell. Transp. Syst.*, **17** (2016), 1956–1967. <https://doi.org/10.1109/TITS.2016.2514271>
16. S. E. Li, Y. Zheng, K. Li, J. Wang, An overview of vehicular platoon control under the four-component framework, in *2015 IEEE Intelligent Vehicles Symposium (IV)*, (2015), 286–291. <https://doi.org/10.1109/IVS.2015.7225700>
17. L. Xiao, F. Gao, Practical string stability of platoon of adaptive cruise control vehicles, *IEEE Trans. Intell. Transp. Syst.*, **12** (2011), 1184–1194. <https://doi.org/10.1109/TITS.2011.2143407>
18. S. Darbha, S. Konduri, P. Pagilla, Benefits of V2V communication for autonomous and connected vehicles, *IEEE Trans. Intell. Transp. Syst.*, **20** (2018), 1954–1963. <https://doi.org/10.1109/TITS.2018.2859765>
19. Y. Zheng, S. E. Li, J. Wang, D. Cao, K. Li, Stability and scalability of homogeneous vehicular platoon: study on the influence of information flow topologies, *IEEE Trans. Intell. Transp. Syst.*, **17** (2015), 14–26. <https://doi.org/10.1109/TITS.2015.2402153>
20. S. E. Li, Y. Zheng, K. Li, Y. Wu, J. K. Hedrick, F. Gao, et al., Dynamical modeling and distributed control of connected and automated vehicles: challenges and opportunities, *IEEE Intell. Transp. Syst. Mag.*, **9** (2017), 46–58. <https://doi.org/10.1109/MITS.2017.2709781>
21. M. Bernardo, P. Falcone, A. Salvi, S. Santini, Design, analysis, and experimental validation of a distributed protocol for platooning in the presence of time-varying heterogeneous delays, *IEEE Trans. Control Syst. Technol.*, **24** (2015), 413–427. <https://doi.org/10.1109/TCST.2015.2437336>

22. S. Stüdli, M. Seron, R. H. Middleton, Vehicular platoons in cyclic interconnections, *Automatica*, **94** (2018), 283–293. <https://doi.org/10.1016/j.automatica.2018.04.033>
23. F. Gao, X. Hu, S. E. Li, K. Li, Q. Sun, Distributed adaptive sliding mode control of vehicular platoon with uncertain interaction topology, *IEEE Trans. Ind. Electron.*, **65** (2018), 6352–6361. <https://doi.org/10.1109/TIE.2017.2787574>
24. F. Gao, S. E. Li, Y. Zheng, D. Kum, Robust control of heterogeneous vehicular platoon with uncertain dynamics and communication delay, *IET Intell. Transp. Syst.*, **10** (2016), 503–513. <https://doi.org/10.1049/iet-its.2015.0205>
25. P. Liu, A. Kurt, U. Ozguner, Distributed model predictive control for cooperative and flexible vehicle platooning, *IEEE Trans. Control Syst. Technol.*, **27** (2018), 1115–1128. <https://doi.org/10.1109/TCST.2018.2808911>
26. A. I. M. Medina, N. V. D. Wouw, H. Nijmeijer, Cooperative intersection control based on virtual platooning, *IEEE Trans. Intell. Transp. Syst.*, **19** (2017), 1727–1740. <https://doi.org/10.1109/TITS.2017.2735628>
27. B. Xu, S. E. Li, Y. Bian, S. Li, X. J. Ban, J. Wang, et al., Distributed conflict-free cooperation for multiple connected vehicles at unsignalized intersections, *Transp. Res. Part C Emerging Technol.*, **93** (2018), 322–334. <https://doi.org/10.1016/j.trc.2018.06.004>
28. Y. Zhou, M. E. Cholette, A. Bhaskar, E. Chung, Optimal vehicle trajectory planning with control constraints and recursive implementation for automated on-ramp merging, *IEEE Trans. Intell. Transp. Syst.*, **20** (2018), 3409–3420. <https://doi.org/10.1109/TITS.2018.2874234>
29. I. Flugge-Lotz, H. Marbach, The optimal control of some attitude control systems for different performance criteria, *J. Fluids Eng.*, **85** (1963), 165–175. <https://doi.org/10.1115/1.3656552>
30. P. Wang, Y. Jiang, L. Xiao, Y. Zhao, Y. Li, A joint control model for connected vehicle platoon and arterial signal coordination, *J. Intell. Transp. Syst.*, **24** (2020), 81–92. <https://doi.org/10.1080/15472450.2019.1579093>
31. J. Gong, J. Cao, Y. Zhao, Y. Wei, J. Guo, W. Huang, Sampling-based cooperative adaptive cruise control subject to communication delays and actuator lags, *Math. Comput. Simul.*, **171** (2020), 13–25. <https://doi.org/10.1016/j.matcom.2019.10.012>
32. Y. Zhao, G. Guo, Distributed tracking control of mobile sensor networks with intermittent communications, *J. Franklin Inst.*, **354** (2017), 3634–3647. <https://doi.org/10.1016/j.jfranklin.2017.03.003>
33. M. A. S. Kamal, M. Mukai, J. Murata, T. Kawabe, Ecological vehicle control on roads with up-down slopes, *IEEE Trans. Intell. Transp. Syst.*, **12** (2011), 783–794. <https://doi.org/10.1109/TITS.2011.2112648>
34. B. Paden, S. Sastry, A calculus for computing Filippov's differential inclusion with application to the variable structure control of robot manipulators, *IEEE Trans. Circuits Syst.*, **34** (1987), 73–82. <https://doi.org/10.1109/TCS.1987.1086038>
35. S. Li, X. Qin, Y. Zheng, J. Wang, K. Li, H. Zhang, Distributed platoon control under topologies with complex eigenvalues: stability analysis and controller synthesis, *IEEE Trans. Control Syst. Technol.*, **27** (2017), 206–220. <https://doi.org/10.1109/TCST.2017.2768041>

---

**Appendix**
**Appendix A**

*Proof of Theorem 1.* Choose the following Lyapunov function for the vehicular platoon system (3.5):

$$V(t) = Z^T(t)(L_N \otimes P^{-1})Z(t) \quad (\text{A1})$$

where  $P > 0$ . Based on the graph theorem,  $L_N > 0$ . Obviously,  $V(t)$  is positive and continuously differentiable. According to [34], if Lebesgue measurable  $f$  is continuous,  $\kappa[f] = \{f\}$ , where  $\kappa[f]$  denotes the intersection over all sets of Lebesgue measure zero. Taking the set-valued Lie derivative along the trajectories of the system (2.10), we have

$$\begin{aligned} \dot{V}(t) = & Z^T(L_N \otimes (P^{-1}A + A^T P^{-1}) + 2\theta_1 L_N^2 \otimes P^{-1}BK)Z \\ & + 2\theta_2 Z^T(L_N \otimes P^{-1}B) \text{sgn}((L_N \otimes K)Z) - \\ & 2Z^T(L_N \mathbf{1} \otimes P^{-1}B)u_0 \end{aligned} \quad (\text{A2})$$

By introducing the state transformation  $\tilde{Z}(t) = (L_N \otimes P^{-1})Z(t)$ , and substituting  $K = -B^T P^{-1}$  into (A2) with the fact that  $x^T \text{sgn}(x) = \|x\|_1$ , we can obtain that

$$\begin{aligned} \dot{V}(t) = & \tilde{Z}^T(L_N \otimes (AP + PA^T) - 2\theta_1 L_N^2 \otimes BB^T)\tilde{Z} \\ & - 2\theta_2 \|(L_N \otimes B^T)\tilde{Z}\|_1 - 2\tilde{Z}^T(L_N \mathbf{1} \otimes B)u_0 \end{aligned} \quad (\text{A3})$$

Based on Holder's inequality  $\|fg\|_1 \leq \|f\|_1 \|g\|_\infty$ , it thus yields

$$\begin{aligned} \dot{V}(t) \leq & \tilde{Z}^T(L_N \otimes (AP + PA^T) - 2\theta_1 L_N^2 \otimes BB^T)\tilde{Z} \\ & - 2(\theta_2 - \omega) \|(L_N \otimes B^T)\tilde{Z}\|_1 \end{aligned} \quad (\text{A4})$$

Choose the parameter  $\theta_2$  with  $\theta_2 \geq \omega$ , and introduce another state transformation  $\hat{Z}(t) = (Q^T \otimes I_N)\tilde{Z}(t)$ , where  $Q$  is an orthogonal matrix such that  $Q^T L_N Q = \Lambda = \text{diag}\{\lambda_1, \dots, \lambda_N\}$ ,  $\lambda_i > 0$ . Then, the following inequation can be derived as:

$$\begin{aligned} \dot{V}(t) \leq & \hat{Z}^T(\Lambda \otimes (AP + PA^T) - 2\theta_1 \Lambda^2 \otimes BB^T)\hat{Z} \\ = & \sum_{i=1}^N \lambda_i \hat{Z}_i^T (AP + PA^T - 2\theta_1 \lambda_i BB^T) \hat{Z}_i \end{aligned} \quad (\text{A5})$$

Let coupling strength satisfy  $\theta_1 \geq 1/\min\{\lambda_i\}$ ,  $i = 1, \dots, N$ . Based on Lemma 1, we have

$$\begin{aligned} \dot{V}(t) \leq & \sum_{i=1}^N \lambda_i \hat{Z}_i^T (AP + PA^T - 2BB^T) \hat{Z}_i \\ < & \sum_{i=1}^N \lambda_i \hat{Z}_i^T (-2\alpha P) \hat{Z}_i \\ = & -2\alpha Z^T(L_N \otimes P^{-1})Z = -2\alpha V(t) \end{aligned} \quad (\text{A6})$$

According to the Comparison lemma [35], it is obtained from (A6) that  $V(t) < e^{-2\alpha t}V(0)$ . Then,

$$\lambda_{\min}(L_N \otimes P^{-1})\|Z(t)\|_2^2 < e^{-2\alpha t}\lambda_{\max}(L_N \otimes P^{-1})\|Z(0)\|_2^2 \quad (\text{A7})$$

Therefore, it yields

$$\|Z(t)\|_2 < \rho e^{-\alpha t}\|Z(0)\|_2 \quad (\text{A8})$$

where  $\rho = \sqrt{\frac{\lambda_{\max}(L_N)\lambda_{\max}(P^{-1})}{\lambda_{\min}(L_N)\lambda_{\min}(P^{-1})}}$ . The condition (A8) indicates the spacing errors between successive vehicles converge to zero exponentially with a speed faster than  $\exp(-\alpha t)$ . This completes the proof.

## Appendix B

In this appendix, we give an example to construct the algebraic equations of the system that contains the state variables of switching points and control switching time for the case  $\{a_{\min}, 0, a_{\max}\}$  in Figure 5(h). Due to three segments control situation, there exist two control switching time  $t_1$  and  $t_2$ ,  $0 < t_1 < t_2 < t_f$ .

For given performance index (2.5), we have

$$\begin{aligned} \min_{u_0} \int_0^{t_f} (\sigma + |u_0|) dt &= \int_0^{t_1} (\sigma - a_{\min}) dt + \int_{t_1}^{t_2} \sigma dt \\ &\quad + \int_{t_2}^{t_f} (\sigma + a_{\max}) dt \end{aligned} \quad (\text{B1})$$

$$u_0^* = \begin{cases} a_{\min}, & t \in [0, t_1) \\ 0, & t \in [t_1, t_2) \\ a_{\max}, & t \in [t_2, t_f] \end{cases} \quad (\text{B2})$$

For  $t \in [0, t_1)$ ,

$$v^*(t) = v_0 + a_{\min}t \quad (\text{B3})$$

$$s^*(t) = -L + v_0 t + 1/2a_{\min}t^2 \quad (\text{B4})$$

For  $t \in [t_1, t_2)$ ,

$$v^*(t) = v_{t1} = v_{t2} \quad (\text{B5})$$

$$s^*(t) = s_{t1} + v_{t1}(t - t_1) \quad (\text{B6})$$

For  $t \in [t_2, t_f)$ ,

$$v^*(t) = v_{t2} + a_{\max}(t - t_2) \quad (\text{B7})$$

$$s^*(t) = s_{t2} + v_{t2}(t - t_2) + 1/2a_{\max}(t - t_2)^2 \quad (\text{B8})$$

At  $t = t_1$ , we have

$$v_{t1} = v_{t2} = v_0 + a_{\min}t_1 \quad (\text{B9})$$

$$s_{t1} = -L + v_0 t_1 + 1/2a_{\min}t_1^2 \quad (\text{B10})$$

At  $t = t_2$ , we have

$$v_{t2} = v_{tf} - a_{max}(t_f - t_2) \quad (\text{B11})$$

$$s_{t2} - s_{t1} = v_{t1}(t_2 - t_1) \quad (\text{B12})$$

$$s_{t2} = -v_{t1}(t_f - t_2) - 1/2a_{max}(t_f - t_2)^2 \quad (\text{B13})$$

Combining the constraint of the arrival time in (2.11), we have six evaluated variables,  $v_{t1}$ ,  $t_1$ ,  $t_2$ ,  $s_{t1}$ ,  $s_{t2}$  and  $t_f$ ; five nonlinear algebraic equations, (B9) through (B13); and one inequality (Eq 2.11). Note that some inequality constraints are naturally required, such as

$$0 < t_1 < t_2 < t_f \quad (\text{B14})$$

$$-L < s_{t1} < s_{t2} < 0 \quad (\text{B15})$$

Thus, we can formulate the optimal control issue as linear and nonlinear programming problems, which can be solved by the “fmincon” function of MATLAB.



AIMS Press

© 2023 the Author(s), licensee AIMS Press. This is an open access article distributed under the terms of the Creative Commons Attribution License (<http://creativecommons.org/licenses/by/4.0>)